



## 저작자표시 2.0 대한민국

이용자는 아래의 조건을 따르는 경우에 한하여 자유롭게

- 이 저작물을 복제, 배포, 전송, 전시, 공연 및 방송할 수 있습니다.
- 이차적 저작물을 작성할 수 있습니다.
- 이 저작물을 영리 목적으로 이용할 수 있습니다.

다음과 같은 조건을 따라야 합니다:



저작자표시. 귀하는 원저작자를 표시하여야 합니다.

- 귀하는, 이 저작물의 재이용이나 배포의 경우, 이 저작물에 적용된 이용허락조건을 명확하게 나타내어야 합니다.
- 저작권자로부터 별도의 허가를 받으면 이러한 조건들은 적용되지 않습니다.

저작권법에 따른 이용자의 권리는 위의 내용에 의하여 영향을 받지 않습니다.

이것은 [이용허락규약\(Legal Code\)](#)을 이해하기 쉽게 요약한 것입니다.

[Disclaimer](#) 

# Comparison of Piezo1-mediated relaxation in the mesenteric resistance arteries in diabetic and control mice

Chae Eun Haam

Department of Medicine

The Graduate School, Yonsei University

# Comparison of Piezo1-mediated relaxation in the mesenteric resistance arteries in diabetic and control mice

Directed by Professor Young-Ho Lee

The Doctoral Dissertation  
submitted to the Department of Medicine,  
the Graduate School of Yonsei University  
in partial fulfillment of the requirements for the degree of  
Doctor of Philosophy in Medical Science

Chae Eun Haam

December 2023

This certifies that the Doctoral Dissertation of  
Chae Eun Haam is approved.

-----  
Thesis Supervisor : Young-Ho Lee

-----  
Thesis Committee Member#1 : Duck-Sun Ahn

-----  
Thesis Committee Member#2 : Inkyeom Kim

-----  
Thesis Committee Member#3 : Seungsoo Chung

-----  
Thesis Committee Member#4 : Soo-Kyung Choi

The Graduate School  
Yonsei University

December 2023

## TABLE OF CONTENTS

<b>LIST OF ABBREVIATIONS</b> .....	
<b>ABSTRACT</b> .....	
<b>I. INTRODUCTION</b> .....	1
<b>II. MATERIALS AND METHODS</b> .....	3
1. Drugs and chemicals .....	3
2. Experimental animals .....	3
3. Blood pressure and blood glucose measurements .....	4
4. Tissue preparation .....	4
5. Measurements of isometric tension .....	4
6. Experimental protocols .....	5
7. Western blot analysis .....	6
8. Immunofluorescence staining .....	7
9. Quantification of co-localization .....	8
10. Statistical analysis.....	8
<b>III. RESULTS</b> .....	9
1. Characteristics of the animals .....	9
2. Expression of Piezo1 in mesenteric arteries of control and db <sup>-</sup> /db <sup>-</sup> mice .....	9
3. Relaxation response of ACh and SNP on mesenteric resistance arteries in control and db <sup>-</sup> /db <sup>-</sup> mice .....	13

4. Effect of Yoda1 on vascular contractility in mesenteric arteries of control and db <sup>-</sup> /db <sup>-</sup> mice .....	15
5. Effects of Dooku1 and GsMTx4 on Yoda1-induced relaxation .....	23
6. Effects of L-NNA, ODQ and INDO on Yoda1-induced relaxation .....	26
7. Effects of IK <sub>Ca</sub> and SK <sub>Ca</sub> channel blockers on Yoda1-induced relaxation .....	29
8. Effect of BK <sub>Ca</sub> channel blocker on Yoda1-induced relaxation .....	32
9. Expression of BK <sub>Ca</sub> channel in mesenteric arteries of control and db <sup>-</sup> /db <sup>-</sup> mice .....	35
10. Co-localization of Piezo1 and BK <sub>Ca</sub> channel in mesenteric arteries of control and db <sup>-</sup> /db <sup>-</sup> mice .....	37
<b>IV. DISCUSSION</b> .....	40
<b>V. CONCLUSION</b> .....	44
<b>REFERENCES</b> .....	45
<b>ABSTRACT (IN KOREAN)</b> .....	48
<b>PUBLICATION LIST</b> .....	50

## LIST OF FIGURES

Figure 1. Piezo1 protein expression profiles in mesenteric arteries of db <sup>-</sup> /db <sup>-</sup> mice compared to control mice .....	11
Figure 2. Relaxation response of ACh and SNP on mesenteric resistance arteries in control and db <sup>-</sup> /db <sup>-</sup> mice .....	14
Figure 3. Effect of Yoda1 on vascular contractility in mesenteric arteries of control and db <sup>-</sup> /db <sup>-</sup> mice .....	17
Figure 4. Role of endothelium in Yoda1-induced relaxation of mesenteric arteries .....	19
Figure 5. Effect of Yoda1 treatment on basal tension in mesenteric arteries with and without endothelium. ....	21
Figure 6. Representative traces showing the effect of vehicle (DMSO) on mesenteric artery rings pre-constricted with U46619 .....	22
Figure 7. Effects of Dooku1 and GsMTx4 on Yoda1-induced relaxation .....	24
Figure 8. Effects of L-NNA, ODQ and INDO on Yoda1-induced relaxation .....	27
Figure 9. Effects of IK <sub>Ca</sub> and SK <sub>Ca</sub> channel blockers on Yoda1-induced relaxation .....	30

Figure 10. Effect of BK <sub>Ca</sub> channel blocker on Yoda1-induced relaxation .....	33
Figure 11. Expression level of BK <sub>Ca</sub> channel in mesenteric arteries of control and db <sup>-</sup> /db <sup>-</sup> mice .....	36
Figure 12. Co-localization of Piezo1 channels and BK <sub>Ca</sub> channels in mesenteric arteries of control and db <sup>-</sup> /db <sup>-</sup> mice .....	38

## LIST OF TABLES

Table 1. Physiological parameters of control and diabetic mice .....	10
--	----

## LIST OF ABBREVIATIONS

ACh	Acetylcholine
SNP	Sodium nitroprusside
NO	Nitric oxide
sGC	Soluble guanylyl cyclase
COX	Cyclooxygenase
L-NNA	N <sup>o</sup> -Nitro-L-arginine
ODQ	1H- [1,2,4]oxadiazolo [4,3,-a]quinoxalin-1-
INDO	Indomethacin
ChTX.	Charybdotoxin
BK <sub>Ca</sub> ,	Large-conductance Ca <sup>2+</sup> -activated K <sup>+</sup>
TRAM-34	Triarylmethane-34
IK <sub>Ca</sub>	Intermediate-conductance Ca <sup>2+</sup> -activated K <sup>+</sup>
SK <sub>Ca</sub>	Small-conductance Ca <sup>2+</sup> -activated K <sup>+</sup>
DMSO	Dimethyl sulfoxide
cGMP	Guanosine 3',5'-cyclic monophosphate
cAMP	Adenosine-3',5'-cyclic monophosphate
W/O	Wash out
SEM	Standard error of the mean
ANOVA	Analysis of variance
PCC	Pearson's correlation coefficient

## ABSTRACT

**Comparison of Piezo1-mediated relaxation in the mesenteric resistance arteries in diabetic and control mice**

Chae Eun Haam

*Department of Medicine  
The Graduate School, Yonsei University*

(Directed by Professor Young-Ho Lee)

Piezo1, a mechanosensitive ion channel, plays a significant role in vascular physiology and disease. However, the involvement of Piezo1 in vascular dysfunction in diabetes remains unclear. This study aims to elucidate the vascular responses and mechanisms elicited by Piezo1 activation. Furthermore, we sought to investigate the differences induced by Piezo1 activation in the arteries of diabetic mice and control mice. Ten- to 12-week-old male C57BL/6 (control) and type 2 diabetic mice (db<sup>-</sup>/db<sup>-</sup>) were used. Second-order mesenteric arteries (~150 μm) were used for isometric tension experiments. Western blot analysis and immunofluorescence staining were conducted to assess protein expression. The expression level of Piezo1 was significantly reduced in the mesenteric arteries of type 2 diabetic mice (db<sup>-</sup>/db<sup>-</sup> mice) compared to control mice (C57BL/6J), as determined through western blot and immunofluorescence staining analysis. The Piezo1 agonist, Yoda1, induced relaxation in mesenteric arteries in a concentration-dependent manner in both control and db<sup>-</sup>/db<sup>-</sup> mice. Interestingly, the relaxation response was notably greater in control mice than in db<sup>-</sup>/db<sup>-</sup> mice. Removal of the endothelium diminished the relaxation responses induced by Yoda1, with a more pronounced effect observed in control mice compared to db<sup>-</sup>/db<sup>-</sup> mice. Pre-treatment with L-NNA (a nitric oxide synthase inhibitor) and ODQ (a soluble guanylate cyclase inhibitor) significantly reduced Yoda1-induced relaxation in both groups. Furthermore, in endothelium-intact arteries of control mice, pre-treatment with apamin (an

SK<sub>Ca</sub> channel blocker), TRAM-34 (an IK<sub>Ca</sub> channel blocker), and charybdotoxin (a BK<sub>Ca</sub> channel blocker) decreased the relaxation response. In endothelium-denuded arteries, pre-incubation with charybdotoxin (a BK<sub>Ca</sub> channel blocker) significantly attenuated Yoda1-induced relaxation in db<sup>-</sup>/db<sup>-</sup> mice, whereas it had no effect in control mice. Co-immunofluorescence staining revealed greater structural coupling between Piezo1 and BK<sub>Ca</sub> channels in db<sup>-</sup>/db<sup>-</sup> mice compared to control mice. These findings suggest that Yoda1-induced relaxation in db<sup>-</sup>/db<sup>-</sup> mice mainly caused by BK<sub>Ca</sub> channel activation in vascular smooth muscle cells. The present study represents the first report detailing the distinctive aspects of vascular responses induced by Piezo1 activation in the mesenteric resistance arteries of type 2 diabetic mice. Our findings have the potential to offer novel insights into the identification of mechanisms that may contribute to vascular dysfunction in diabetes.

---

Key words : piezo1; yoda1; type 2 diabetes; vasorelaxation; mechanotransduction

## **Comparison of Piezo1-mediated relaxation in the mesenteric resistance arteries in diabetic and control mice**

Chae Eun Haam

*Department of Medicine  
The Graduate School, Yonsei University*

(Directed by Professor Young-Ho Lee)

### **I. INTRODUCTION**

Diabetes mellitus is a complex metabolic disorder characterized by hyperglycemia resulting from impaired insulin secretion, defective insulin action, or both.<sup>1</sup> Diabetes is associated with vascular dysfunction, particularly impairments in endothelium-dependent relaxation, which are considered critical in the development of diabetes-induced vascular complications.<sup>2</sup> Endothelial dysfunction is a central event in the pathogenesis of diabetes and significantly influences the development of future vascular complications.<sup>3</sup> However, the mechanisms underlying this damage remain incompletely understood. Therefore, it is crucial to comprehend the mechanisms responsible for endothelial dysfunction caused by diabetes mellitus and to identify treatments that can enhance or restore endothelial function to prevent diabetic vascular complications.

Mechanotransduction, the conversion of mechanical forces into biochemical signals, plays a crucial role in vascular development, physiology, and disease.<sup>4</sup> In 2010, Piezo1, a mechanically-sensitive non-selective cation channel, was identified as an essential protein expressed in endothelial and vascular smooth muscle cells.<sup>5-8</sup> Piezo1 is considered a sensor for shear stress in vascular structures and is crucial for embryonic development.<sup>9</sup>

Furthermore, Piezo1 is required for vasculogenesis, valve morphogenesis, and the regulation of vascular tone.<sup>10,11</sup> Interestingly, Piezo1 exerts atheroprotective effects by regulating nitric oxide (NO) release by the endothelium. Conversely, the activation of Piezo1 through high hydrostatic pressure not only disrupts the barrier function of lung endothelial cells but also leads to arterial remodeling under hypertensive conditions. Additionally, it induces a pro-atherogenic response when exposed to turbulent flow.<sup>12</sup> A previous study by Zhu *et al.* demonstrated that dysregulation of Piezo1 occurs in multiple blood lineages in patients with type 2 diabetes mellitus (T2DM). They also reported that elevated Piezo1 activity induces prothrombotic cellular responses in red blood cells, neutrophils, and platelets. Inhibition of Piezo1 provided protection against thrombosis in zebrafish genetic models and human blood samples, particularly in hyperglycemic conditions.<sup>13</sup>

Although the significance of Piezo1 in vascular function has been studied, no reports have investigated the involvement of Piezo1 in diabetic vascular dysfunction. Therefore, our study sought to elucidate the vascular responses induced by Piezo1 activation in mesenteric resistance arteries in both control and diabetic mice. Additionally, we explored different aspects and mechanisms underlying Piezo1-induced responses in control and diabetic mice.

## II. MATERIALS AND METHODS

### 1. Drugs and chemicals

All drugs and reagents, including Yoda1, were procured from Sigma-Aldrich (St. Louis, MO, USA) unless otherwise specified. U46619 was obtained from Enzo Life Sciences (Farmingdale, NY, USA), and indomethacin was obtained from Calbiochem (Darmstadt, Germany). Dooku1 was acquired from Tocris Bioscience (Bristol, UK), while charybdotoxin (ChTX) was purchased from Alomone Labs (Jerusalem, Israel).

### 2. Experimental animals

Ten- to 12-week-old male C57BL/6 (control) and type 2 diabetic mice (db<sup>-</sup>/db<sup>-</sup>) were purchased from Central Lab Animal Inc. (Seoul, Republic of Korea). All animals were housed in an environmentally controlled room (temperature: 22.0 ± 2°C, humidity: 55 ± 5%, a cycle of 12 h light/dark) and had *ad libitum* access to food and water. All experiments were conducted in accordance with the *Guide for the Care and Use of Laboratory Animals* published by the US National Institutes of Health (NIH publication No. 85-23, 2011), and were approved by the Institutional Animal Care and Use Committees at the Yonsei University College of Medicine (protocol number 2023-0016).

### **3. Blood pressure and blood glucose measurements**

Systolic blood pressure was monitored in the mice trained for 3 days using the non-invasive computerized tail-cuff system (BP-2000, Visitech Systems, Apex, NC, USA). Blood glucose levels were measured from tail vein blood samples following a fasting period of 5–6 hours using an Accu-Chek glucometer (Roche Diagnostic, Berlin, Germany).

### **4. Tissue preparation**

In all experiments, mice were euthanized through isoflurane inhalation. To confirm death, the mice were carefully checked for several signs, such as no response to toe pinch, no palpable heartbeat, and color change opacity in the eyes. The small intestine, along with the attached vasculature, was swiftly excised and submerged in ice-cold Krebs-Henseleit solution (composition in mmol/L: NaCl 119, KCl 4.6, MgSO<sub>4</sub> 1.2, KH<sub>2</sub>PO<sub>4</sub> 1.2, CaCl<sub>2</sub> 2.5, NaHCO<sub>3</sub> 25, and glucose 11.1). The solution was continuously bubbled with a mixture of 95% O<sub>2</sub> and 5% CO<sub>2</sub>. Second-order mesenteric arteries, approximately ~150 μm in diameter, were carefully isolated from surrounding fat and connective tissues. These vessels were then cut into 2–3mm-long rings for use in isometric tension experiments. When necessary, endothelial denudation was achieved by perfusing the vessels with 0.1% Triton X-100 for 10–15 seconds.

### **5. Measurements of isometric tension**

Isolated mesenteric artery rings were mounted on an isometric wire myograph system (620M, Danish Myotechnology, Aarhus, Denmark) using 25 μm wires and allowed to equilibrate for 20 minutes. The vascular rings were stretched to an optimal resting tension of approximately 2.5 mN. After 30 minutes of equilibration, the rings were stimulated

twice with a high  $K^+$  (70 mM) solution (composition in mmol/L: NaCl 53.6, KCl 70,  $MgSO_4$  1.2,  $KH_2PO_4$  1.2,  $CaCl_2$  2.5,  $NaHCO_3$  25 and glucose 11.1) for 3–5 minutes at 10-minute intervals prior to initiating the experiments

## 6. Experimental protocols

Upon inducing contraction with U46619 ( $10^{-6}$  M), concentration-dependent responses to Yoda1 ( $10^{-7}$ – $10^{-5}$  M, a selective Piezo1 activator) were recorded in mesenteric arteries. To investigate whether the vascular endothelium plays a role in the vasodilatory mechanism of Yoda1, we assessed Yoda1 ( $10^{-5}$  M)-induced relaxation in mesenteric artery rings pre-contracted with U46619 ( $10^{-6}$  M), both with and without the vascular endothelium. When required, the endothelium was removed by perfusing with 0.1% Triton X-100 for 10–15 seconds. In control mice, the endothelium was considered denuded if acetylcholine (ACh,  $10^{-5}$  M) induced less than 20% relaxation.

To assess whether Yoda1 ( $10^{-5}$  M) induced relaxation via Piezo1, mesenteric arteries were pre-incubated with Dooku1 ( $5 \times 10^{-6}$  M), a selective Yoda1 inhibitor, and GsMTx4 ( $2 \times 10^{-5}$  M), a selective blocker of mechanosensitive ion channels.

To investigate the involvement of nitric oxide (NO), soluble guanylyl cyclase (sGC), and cyclooxygenase (COX) in Yoda1-induced relaxation, arteries were pre-treated with the following specific inhibitors:  $N^{\omega}$ -Nitro-L-arginine (L-NNA,  $5 \times 10^{-4}$  M), a nitric oxide synthase inhibitor; a soluble guanylyl cyclase (sGC) inhibitor, 1H- [1,2,4]oxadiazolo [4,3,-a] quinoxalin-1-one (ODQ,  $10^{-5}$  M); a cyclooxygenase inhibitor, indomethacin (INDO,  $10^{-5}$  M).

To characterize the K<sup>+</sup> channels responsible for mediating the relaxation induced by Yoda1, arteries were pre-treated with the following agents: charybdotoxin (ChTX, 5×10<sup>-8</sup> M), a BK<sub>Ca</sub> channel blocker; Triarylmethane-34 (TRAM-34, 10<sup>-6</sup> M), an IK<sub>Ca</sub> channel blocker; apamin (5×10<sup>-7</sup> M), an SK<sub>Ca</sub> channel blocker.

The equation used to calculate the degree of relaxation is as follows:

$$\text{Relaxation (\%)} = \{(B - C)/(B - A)\} \times 100$$

In the equation, A represents the resting tension of artery rings before pre-contraction with U46619 (10<sup>-6</sup> M), B is the maximum contraction of artery rings after pre-contraction using U46619, and C is the contraction of the artery rings after the drug treatment.

## 7. Western blot analysis

Mesenteric arteries were homogenized in ice-cold radioimmunoprecipitation assay buffer (RIPA buffer, Thermo Fisher Scientific, Waltham, MA, USA, Cat# 89900) containing a protease/phosphatase inhibitor cocktail (Thermo Fisher Scientific, Cat# 78440). The protein concentration was determined using a bicinchoninic acid (BCA) protein assay kit (Thermo Fisher Scientific, Cat# 23227). Afterward, the loading samples were separated on a 6%–15% sodium dodecyl sulfate-polyacrylamide (SDS) gel and transferred to nitrocellulose membranes. Following a 1hour block with 5% (w/v) skim milk, the membranes were incubated overnight at 4°C with primary antibodies against rabbit anti-Piezo1 (1:200; Alomone Labs, Cat# APC-087) and rabbit anti-KCNMA1 (1:200; [K<sub>Ca</sub> 1.1] Alomone Labs, Jerusalem, Israel, Cat# APC-151), followed by incubation with horseradish peroxidase-conjugated secondary antibody (1:5000; Santa

Cruz Biotechnology, Dallas, TX, USA, Cat# sc-2357). Protein bands were visualized using the SuperSignal West Pico plus chemiluminescent substrate (Thermo Fisher Scientific, Cat# 34557). In the case of phosphorylated proteins, membranes were stripped with Restore™ Western Blot Stripping Buffer (Thermo Fisher Scientific, Cat # 21059) and reprobed for total protein analysis. The density of  $\beta$ -actin bands from the same blots was used to normalize the target band for quantitative analysis.

## **8. Immunofluorescence staining**

Immunofluorescence staining was conducted to detect the expression of Piezo1 and BK<sub>Ca</sub> channels in the collected mesenteric arteries from both control and type 2 diabetic mice. The tissue was embedded in OCT (optimal cutting temperature) compound and snap-frozen with liquid nitrogen (LN2) before being stored at  $-80\text{ }^{\circ}\text{C}$  until further processing. Fresh-frozen sections,  $4\text{ }\mu\text{m}$  thick, were obtained using a cryostat. These sections were subsequently washed in Tris-buffered saline with Tween20 (TBST) and then blocked with 5% (w/v) bovine serum albumin (BSA) for 1 hour to minimize nonspecific binding. Following the blocking step, the sections were incubated overnight at  $4\text{ }^{\circ}\text{C}$  with a 1:100 dilution of the following primary antibodies: mouse anti-Piezo1 (Thermo Fisher Scientific, Cat# MA5-32876) and rabbit anti-KCNMA1 ([K<sub>Ca</sub> 1.1] Alomone Labs, Jerusalem, Israel, Cat# APC-151). Next, the sections were treated with a 1:100 dilution of secondary antibodies [Alexa Fluor 594-conjugated donkey anti-mouse IgG (Cat# A-32744) and Alexa Fluor 488-conjugated donkey anti-rabbit IgG (Cat# A-32790)] from Invitrogen (Thermo Fisher Scientific) for 1 hour at room temperature in the dark. The sections were mounted in VECTASHIELD Mounting Medium with DAPI (Vector laboratories, Peterborough, UK, Cat# H-120010). Fluorescence imaging of the

stained sections was conducted using laser-scanning confocal microscopy (LSM710, Carl Zeiss, Germany).

## **9. Quantification of co-localization**

Pearson's correlation coefficient (PCC) was employed for quantitative analysis of colocalization using the JACoP tool in ImageJ. The PCC is a statistical measure used to evaluate the overall association between two probes within an image, thus providing an indirect means to quantify their degree of colocalization. The scale of the PCC ranges from  $-1$  to  $1$ , where  $1$  represents strong colocalization,  $-1$  indicates negative colocalization, and  $0$  signifies no colocalization.

## **10. Statistical analysis**

The normal distribution of data was confirmed using the Shapiro–Wilk test. Data are presented as mean  $\pm$  standard error of the mean (SEM) for the number of arteries derived from each distinct animal ( $n$ ), except for pooled samples. One-way or two-way ANOVA was employed to compare the groups, followed by multiple comparison testing using Bonferroni post-hoc tests. P-values  $< 0.05$  were considered statistically significant. Statistical analysis was conducted using GraphPad Prism Version 10.0.0 (GraphPad Software Inc., San Diego, CA, USA).

### **III. RESULTS**

#### **1. Characteristics of the animals**

The body weight was significantly higher in  $db^{-}/db^{-}$  mice compared to C57BL/6 (control) mice, and blood glucose levels were markedly elevated in  $db^{-}/db^{-}$  mice compared to the control mice. However, there was no significant difference in systolic blood pressure between  $db^{-}/db^{-}$  and control mice (Table 1).

#### **2. Expression of Piezo1 in mesenteric arteries of control and $db^{-}/db^{-}$ mice**

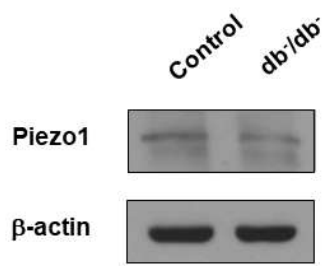
First, we investigated whether Piezo1 is expressed in the mesenteric arteries of both control and  $db^{-}/db^{-}$  mice. Our western blot analysis revealed a significantly lower expression level of Piezo1 in  $db^{-}/db^{-}$  mice compared to control mice (Fig. 1A and B). To further visualize Piezo1 expression, we conducted immunofluorescence staining using Piezo1 (red) and DAPI (nuclei, blue). The fluorescence signal of Piezo1 (red) was weaker in  $db^{-}/db^{-}$  mice compared to control mice (Fig. 1C).

**Table 1.** Physiological parameters of control and diabetic mice

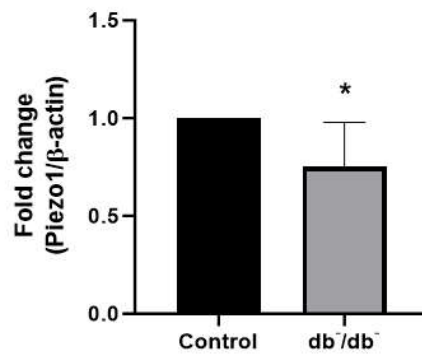
	<b>Control (C57BL/6J)</b>	<b>Diabetic (db<sup>-</sup>/db<sup>-</sup>)</b>
<b>Blood glucose (mg/dL)</b>	123±3.6	573.5±9.2****
<b>Body weight (g)</b>	25.8±0.3	40.6±0.3****
<b>Systolic blood pressure (mmHg)</b>	107±2.3	109±2.1

\*\*\*\*  $p < 0.0001$ , C57BL/6J vs. db<sup>-</sup>/db<sup>-</sup>. means ± SEM. Blood glucose and blood pressure, n=6 for each group. Body weight, n=10 for each group.

A



B



C

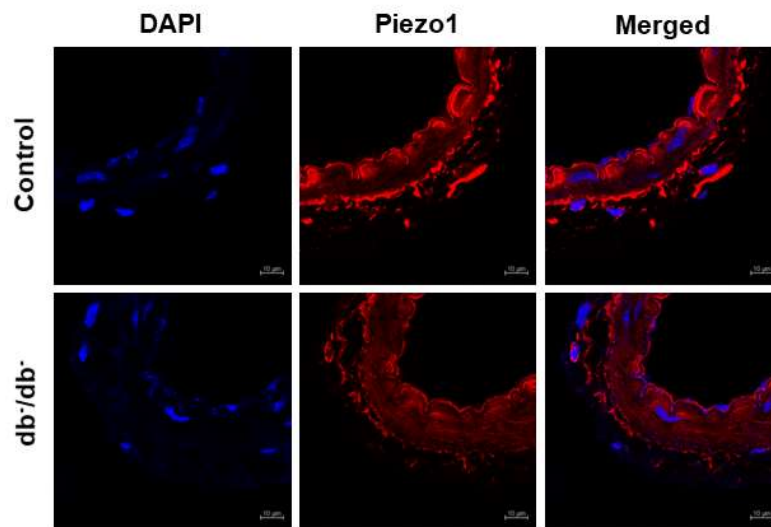


**Figure 1.** Piezo1 protein expression profiles in mesenteric arteries of db/db mice compared to control mice. Representative images (**A**) and summarized data (**B**) showing Piezo1 expression level and evaluated using western blotting.  $\beta$ -actin was used as a loading control. Protein fold-changes are displayed as the ratio of the Piezo1 protein band to the  $\beta$ -actin protein band. The data are presented as mean  $\pm$  SEM (n = 4). \* $p$  < 0.05, control vs. db/db. (**C**) Representative images of immunofluorescence staining of Piezo1 (red) and DAPI (nuclei, blue).

### **3. Relaxation response of ACh and SNP on mesenteric resistance arteries in control and db<sup>-/-</sup> mice**

We next generated dose-response curves for acetylcholine (ACh,  $10^{-9}$ – $10^{-5}$  M) and sodium nitroprusside (SNP,  $10^{-9}$ – $10^{-4}$  M). The endothelium-dependent relaxation (EDR) induced by ACh was significantly reduced in U46619 ( $10^{-6}$  M)-contracted mesenteric arteries of db<sup>-/-</sup> mice. In contrast, endothelium-independent relaxation induced by SNP showed no significant differences between the two groups at the measured concentrations, except for the  $10^{-7}$  M concentration (Fig. 2).

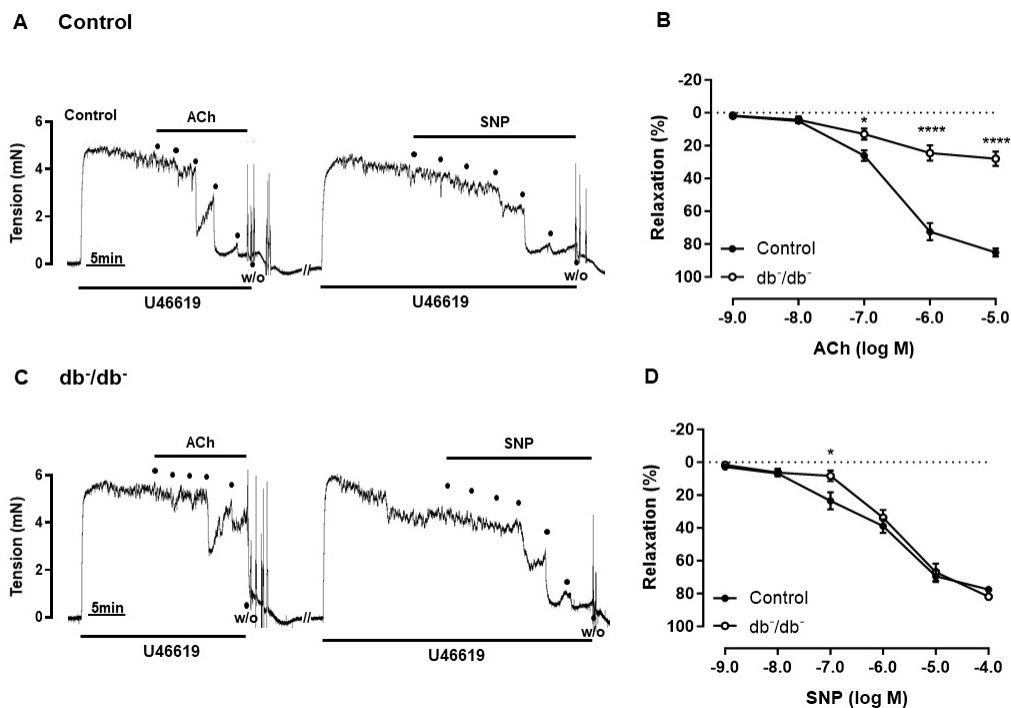


**Figure 2.** Relaxation response of ACh and SNP on mesenteric resistance arteries in control and  $db/db$  mice. Representative traces and curves illustrating the ACh-induced endothelium-dependent relaxation (A and B) and SNP-induced endothelium-independent relaxation (C and D) in mesenteric arteries of control and  $db/db$  mice. The data are presented as means  $\pm$  SEM;  $n = 8$  for control,  $n = 8$  for  $db/db$  (A–D); \* $p < 0.05$ , \*\*\*\* $p < 0.0001$ , control vs.  $db/db$ . ACh, acetylcholine; SNP, sodium nitroprusside; W/O, wash out.

#### **4. Effect of Yoda1 on vascular contractility in mesenteric arteries of control and db<sup>-/-</sup>/db<sup>-/-</sup> mice**

To investigate the impact of Piezo1 activation, we assessed the effect of Yoda1, a selective Piezo1 activator, on vascular contractility in isolated mesenteric artery segments from both control (C57BL/6) and diabetic mice (db<sup>-/-</sup>/db<sup>-/-</sup>). Yoda1 was administered at concentrations ranging from 10<sup>-7</sup> to 10<sup>-5</sup> M. Activation of the Piezo1 by Yoda1 (10<sup>-7</sup>–10<sup>-5</sup> M) induced a concentration-dependent relaxation response in both control (Fig. 3A) and db<sup>-/-</sup>/db<sup>-/-</sup> mice (Fig. 3C). Notably, this relaxation response was attenuated in db<sup>-/-</sup>/db<sup>-/-</sup> mice compared to control mice (Fig. 3A and C). To assess the contribution of endothelium to Yoda1-induced relaxation, we performed experiments using endothelium-intact and endothelium-denuded artery rings. Yoda1-induced relaxation was significantly decreased in endothelium-denuded arteries in control (Fig. 3A and B) and db<sup>-/-</sup>/db<sup>-/-</sup> mice (especially at concentrations of 10<sup>-6.5</sup> M, 10<sup>-6</sup> M, and 10<sup>-5</sup> M, Fig. 3C and D). Interestingly, the removal of the endothelium decreased relaxation responses induced by Yoda1, and this effect was more pronounced in control mice than in db<sup>-/-</sup>/db<sup>-/-</sup> mice. (Fig. 3B and D).

Based on the concentration-response curve, subsequent experiments utilized a Yoda1 concentration of 10<sup>-5</sup> M. Endothelium-intact (Endo+) or endothelium-denuded (Endo-) arteries were pre-contracted with U46619 (10<sup>-6</sup> M) and subsequently treated with Yoda1 at a concentration of 10<sup>-5</sup> M, which elicited the maximum relaxation effect. Yoda1 (10<sup>-5</sup> M) induced relaxation responses in endothelium-intact arteries in both control and db<sup>-/-</sup>/db<sup>-/-</sup> mice. Consistent with the concentration-response results in Fig. 3, the relaxation response induced by Yoda1 was greater in control mice than in db<sup>-/-</sup>/db<sup>-/-</sup> mice (Fig. 4A and B). Removal of the endothelium significantly reduced Yoda1-induced relaxation responses in both control and db<sup>-/-</sup>/db<sup>-/-</sup> mice (Fig. 4C and D). Interestingly, endothelial

removal had a greater effect in control mice (Endo+:  $40.9 \pm 0.8\%$  vs. Endo-:  $10.9 \pm 1.1\%$ , approximately 30% of reduction) than in db/db<sup>-</sup> mice (Endo+:  $34.4 \pm 1.0\%$  vs. Endo-:  $23.7 \pm 2.2\%$ , approximately 10% of reduction). Treating the vessels with Yoda1 ( $10^{-7}$ – $10^{-5}$  M), either with or without endothelium, had no effect on basal tension (Fig. 5). The vehicle, dimethyl sulfoxide (DMSO, 0.015%–0.150%), had no effect on U46619-induced contracted rings when compared to treatment with Yoda1 (Fig. 6A and B).

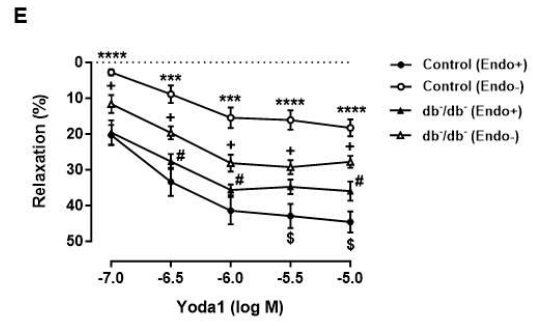
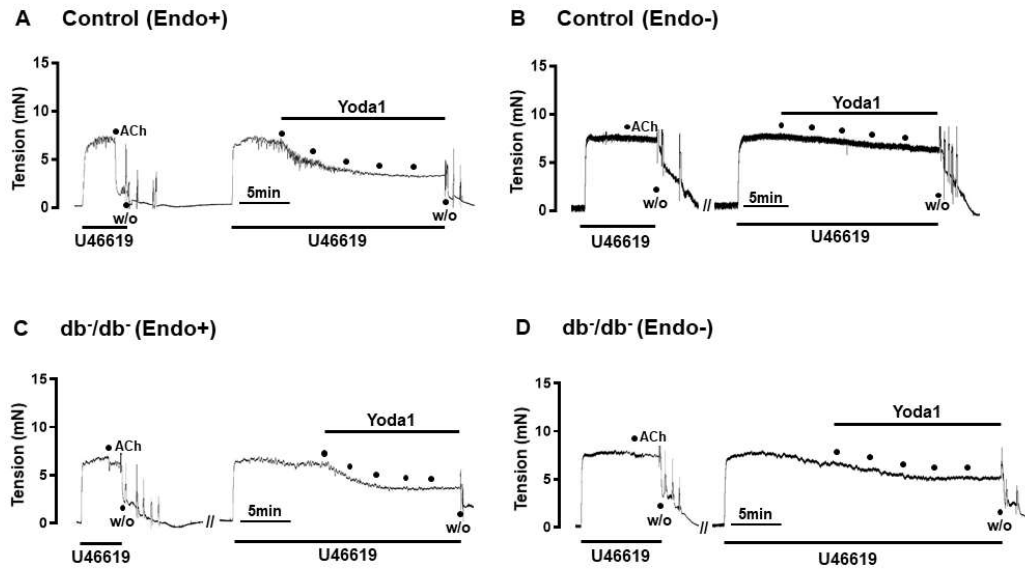
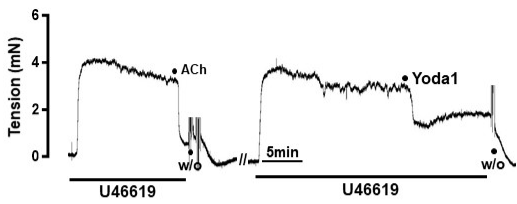
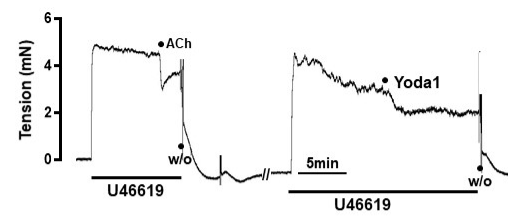


**Figure 3.** Effect of Yoda1 on vascular contractility in mesenteric arteries of control and db/db mice. Representative traces showing the effects of Yoda1 ( $10^{-7}$ – $10^{-5}$  M) in endothelium-intact (Endo+) and endothelium-denuded (Endo-) mesenteric arteries of control (A and B) and db/db mice (C and D). Summarized graph (E) showing the relaxation responses induced by Yoda1 ( $10^{-7}$ – $10^{-5}$  M) in endothelium-intact and endothelium-denuded mesenteric arterial rings of control and db/db mice. The data are presented as means  $\pm$  SEM; n = 7 for control (Endo+), n = 7 for control (Endo-), n=8 for db/db (Endo+), n = 7 for db/db (Endo-). \*\*\* $p$  < 0.001, \*\*\*\* $p$  < 0.0001, control (Endo+) vs. control (Endo-), # $p$  < 0.05, db/db (Endo+) vs. db/db (Endo-), § $p$  < 0.05, control (Endo+) vs. db/db (Endo+), + $p$  < 0.05, control (Endo-) vs. db/db (Endo-). W/O, wash out.

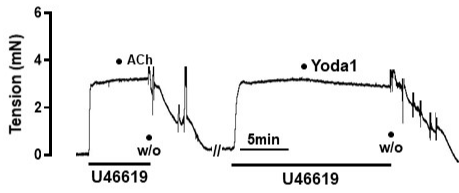
**A Control (Endo+)**



**B db/db<sup>-</sup> (Endo+)**



**C Control (Endo-)**



**D db/db<sup>-</sup> (Endo-)**

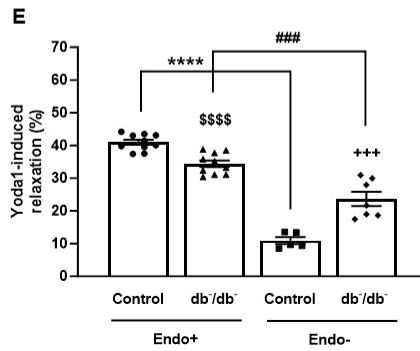
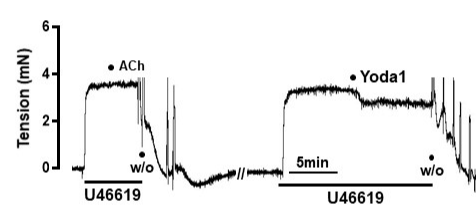


**Figure 4.** Role of endothelium in Yoda1-induced relaxation of mesenteric arteries. Representative recordings showing Yoda1-induced relaxation in endothelium-intact (Endo+) or endothelium-denuded (Endo-) mesenteric artery rings in control (A and C) and db<sup>-</sup>/db<sup>-</sup> mice (B and D). Summarized data (E) of Yoda1-induced relaxation with endothelium (Endo+), and without endothelium (Endo-). The data are presented as means  $\pm$  SEM; n = 10 for control (Endo+), n=10 for db<sup>-</sup>/db<sup>-</sup> (Endo+), n = 5 for control (Endo-), n = 7 for db<sup>-</sup>/db<sup>-</sup> (Endo-). \*\*\*\* $p$  < 0.0001, control (Endo+) vs. control (Endo-), ### $p$  < 0.001, db<sup>-</sup>/db<sup>-</sup> (Endo+) vs. db<sup>-</sup>/db<sup>-</sup> (Endo-), \$\$\$\$ $p$  < 0.0001, control (Endo+) vs. db<sup>-</sup>/db<sup>-</sup> (Endo+), +++ $p$  < 0.001, control (Endo-) vs. db<sup>-</sup>/db<sup>-</sup> (Endo-). ACh, acetylcholine; W/O, wash out

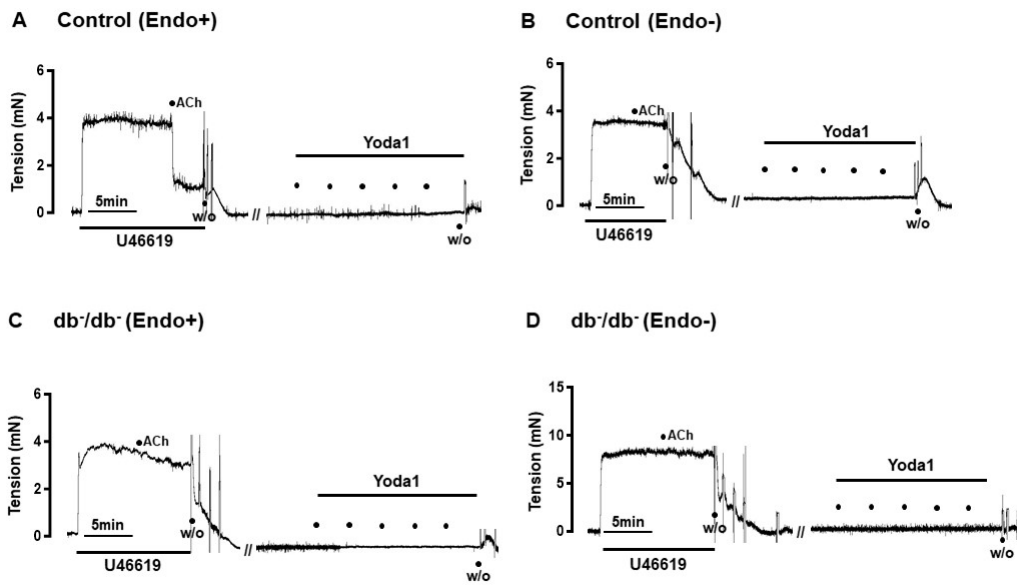


**Figure 5.** Effect of Yoda1 treatment on basal tension in mesenteric arteries with and without endothelium. Representative traces showing response to cumulative concentrations of Yoda1 ( $10^{-7}$ – $10^{-5}$  M) to basal tension of endothelium-intact and endothelium-denuded arteries of control and  $db^{-}/db^{-}$  mice. ACh, acetylcholine; W/O, wash out.

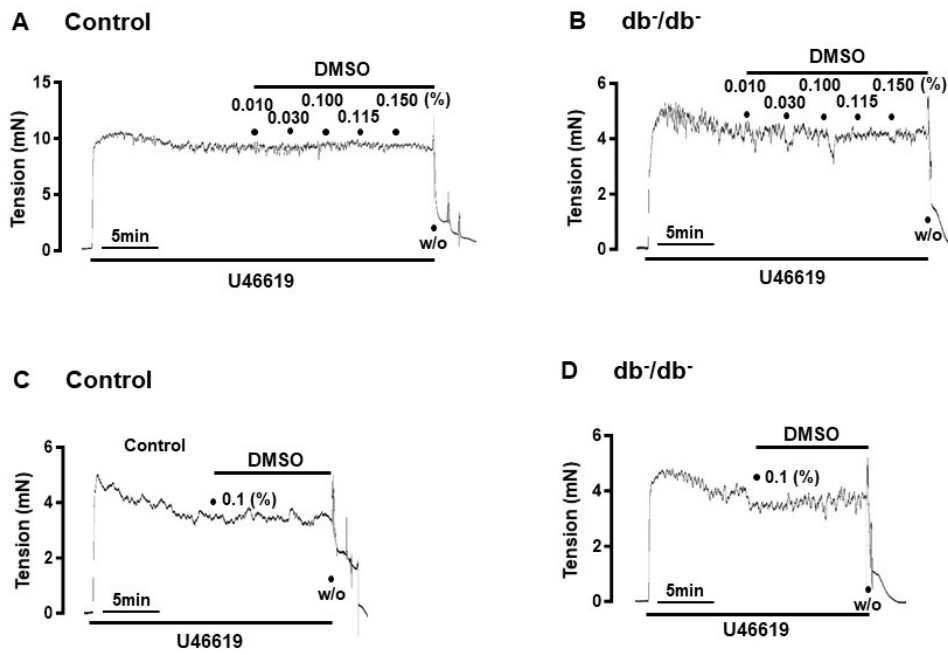
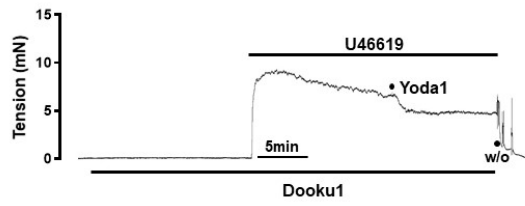


**Figure 6.** Representative traces showing the effect of vehicle (DMSO) on mesenteric artery rings pre-constricted with U46619. DMSO, dimethyl sulfoxide; W/O, wash out.

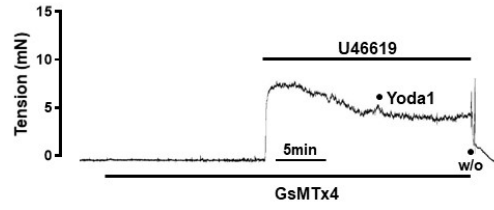
## 5. Effects of Dooku1 and GsMTx4 on Yoda1-induced relaxation

As illustrated in Fig. 4E and F, Yoda1-induced relaxation was measured at  $40.9 \pm 0.8\%$  in control mice and  $34.4 \pm 1.0\%$  in  $db^{-}/db^{-}$  mice. Pre-treatment with Dooku1 (a selective inhibitor of Yoda1) and GsMTx4 (mechanosensitive channel-selective inhibitor) significantly reduced Yoda1-induced relaxation in both control ( $23.1 \pm 2.3\%$  and  $10.7 \pm 2.7\%$ , respectively, Fig. 7A and B) and  $db^{-}/db^{-}$  mice ( $11.8 \pm 3.6\%$  and  $0.4 \pm 4.1\%$ , respectively, Fig. 7C and D). These findings demonstrate that Yoda1 exhibits specificity for the Piezo1 channel (Fig. 7). The vehicle, DMSO (0.1%), had no impact on U46619-induced contracted rings when compared to treatment with Yoda1 (Fig. 6C and D).

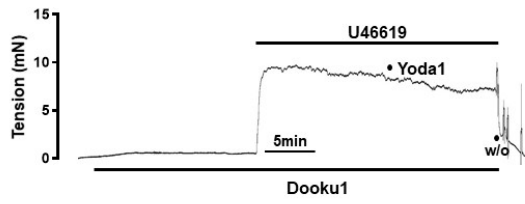
**A Control**



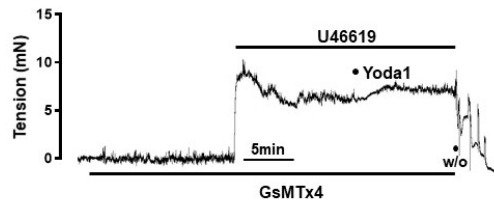
**B Control**



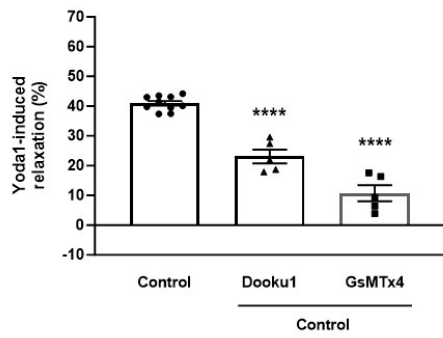
**C db/db<sup>-</sup>**



**D db/db<sup>-</sup>**



**E**



**F**

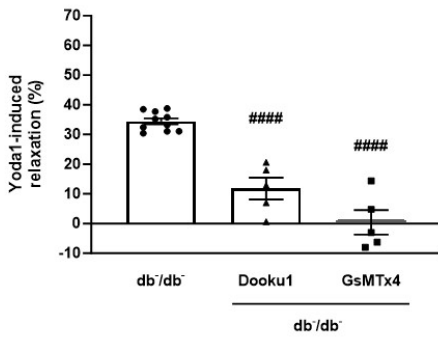
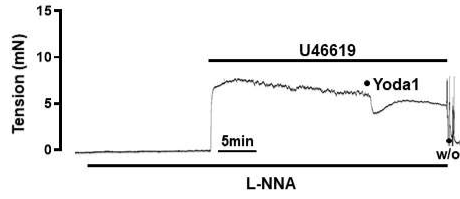


**Figure 7.** Effects of Dooku1 and GsMTx4 on Yoda1-induced relaxation. Representative traces showing the effects of Yoda1 ( $10^{-5}$  M) in the presence of Dooku1 ( $5 \times 10^{-6}$  M) or GsMTx4 ( $2 \times 10^{-5}$  M) in mesenteric arteries of control (A and B) and db<sup>-</sup>/db<sup>-</sup> mice (C and D). Summarized data (E and F) of Yoda1-induced relaxation (%) with or without Dooku1 and GsMTx4. Relaxation (%) indicates the percentage of U46619 ( $10^{-6}$  M)-induced contraction. The data are presented as means  $\pm$  SEM; n = 5 for control (Dooku1), n = 5 for control (GsMTx4), n=5 for db<sup>-</sup>/db<sup>-</sup> (Dooku1), n = 7 for db<sup>-</sup>/db<sup>-</sup> (GsMTx4). \*\*\*\**p* < 0.0001 vs. control, ##### *p* < 0.0001 vs. db<sup>-</sup>/db<sup>-</sup>. W/O, wash out.

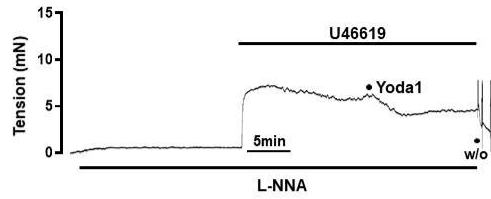
## 6. Effects of L-NNA, ODQ and INDO on Yoda1-induced relaxation

In both control and db<sup>-</sup>/db<sup>-</sup> mice, pre-treatment with N<sup>ω</sup>-Nitro-L-arginine (L-NNA), a nitric oxide synthase inhibitor, significantly decreased Yoda1-induced relaxation compared to the untreated group (Fig. 8A and B). In control mice, the relaxation response decreased from  $40.9 \pm 0.8\%$  to  $18.1 \pm 1.2\%$  after pre-treatment with L-NNA. In db<sup>-</sup>/db<sup>-</sup> mice, the relaxation response decreased from  $34.4 \pm 1.0\%$  to  $23.6 \pm 3.9\%$  following pre-incubation with L-NNA. Similarly, pre-incubation with ODQ, a soluble guanylate cyclase (sGC) inhibitor, also resulted in a significant reduction in Yoda1-induced relaxation in both control and db<sup>-</sup>/db<sup>-</sup> mice (Fig. 8C and D). In control mice, the Yoda1-induced relaxation response decreased from  $40.9 \pm 0.8\%$  to  $31.0 \pm 1.1\%$  following pre-treatment with ODQ. In db<sup>-</sup>/db<sup>-</sup> mice, the Yoda1-induced relaxation response decreased from  $34.4 \pm 1.0\%$  to  $29.7 \pm 2.6\%$  after pre-treatment with ODQ. However, pre-treatment with indomethacin (INDO), a cyclooxygenase (COX) inhibitor, showed no significant difference in Yoda1-induced relaxation in both groups (Fig. 8E and F).

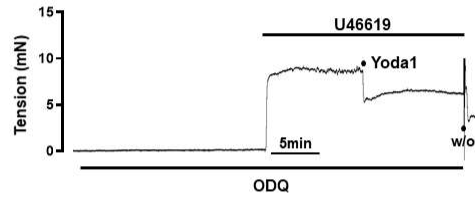
**A Control**



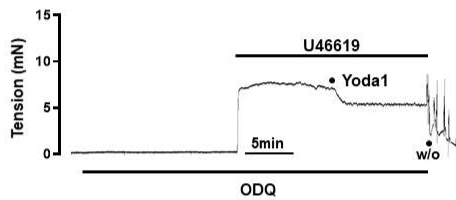
**B db/db<sup>-</sup>**



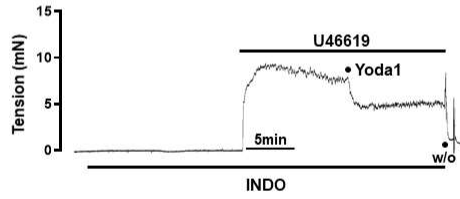
**C Control**



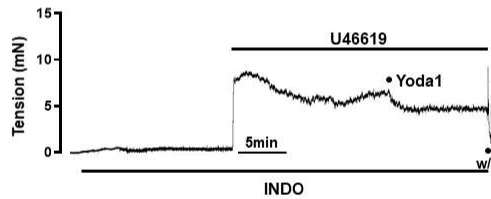
**D db/db<sup>-</sup>**



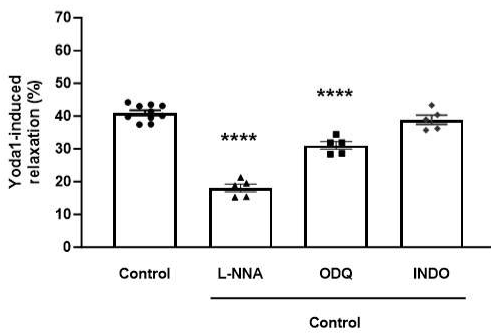
**E Control**



**F db/db<sup>-</sup>**



**G**



**H**

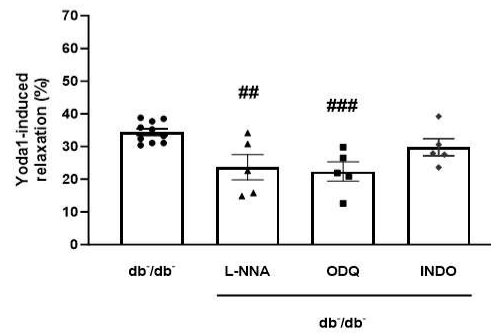
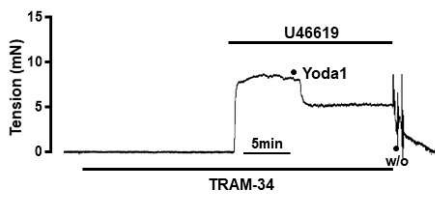


**Figure 8.** Effects of L-NNA, ODQ, and INDO on Yoda1-induced relaxation. Representative original traces of Yoda1-induced relaxation with L-NNA (A and B), ODQ (C and D), or INDO (E and F) in control and db<sup>-/-</sup> mice. The data in G and H represent mean  $\pm$  SEM values of Yoda1-induced relaxation observed in the control (G) and db<sup>-/-</sup> mice (H). n = 5 for control (L-NNA), n=5 for db<sup>-/-</sup> (L-NNA), n = 5 for control (ODQ), n = 5 for db<sup>-/-</sup> (ODQ), n = 5 for control (INDO), n = 5 for db<sup>-/-</sup> (INDO). \*\*\*\**p* < 0.0001 vs. control, ##*p* < 0.01, ####*p* < 0.001 vs. db<sup>-/-</sup>. L-NNA, N<sup>o</sup>-Nitro-L-arginine; ODQ, 1H-[1,2,4]oxadiazolo [4,3,-a] quinoxalin-1-one; INDO, indomethacin; W/O, wash out.

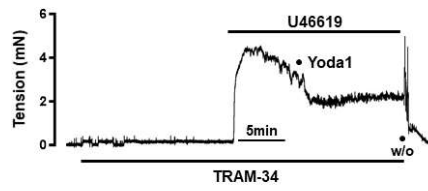
## 7. Effects of $IK_{Ca}$ and $SK_{Ca}$ channel blockers on Yoda1-induced relaxation

Our study explored whether  $IK_{Ca}$  and  $SK_{Ca}$  channels are involved in Yoda1-induced relaxation. In control mice, the relaxation response to Yoda1 was modestly inhibited in the presence of TRAM-34 ( $10^{-6}$  M), an  $IK_{Ca}$  channel blocker, and apamin ( $5 \times 10^{-7}$  M), an  $SK_{Ca}$  channel blocker. Yoda1-induced relaxation decreased from  $40.9 \pm 0.8\%$  to  $36.4 \pm 1.8\%$  after pre-treatment with TRAM-34 (Fig. 9A). The relaxation (%) to Yoda1 before and after apamin treatment was determined to be  $40.9 \pm 0.8\%$  and  $34.0 \pm 2.8\%$ , respectively (Fig. 9C). However, in  $db^{-}/db^{-}$  mice, TRAM-34 and apamin did not affect Yoda1-induced relaxation (Fig. 9B and D).

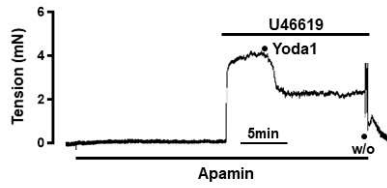
**A Control**



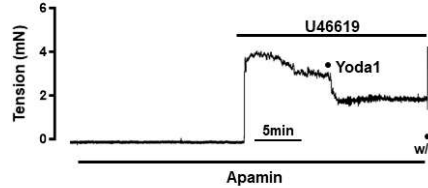
**B db/db<sup>-</sup>**



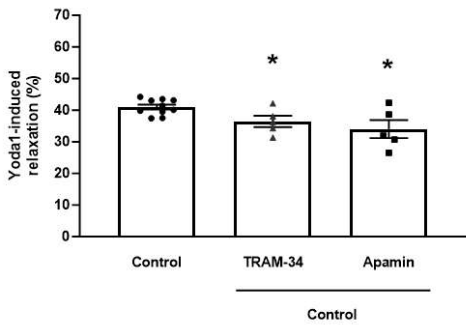
**C Control**



**D db/db<sup>-</sup>**



**E**



**F**

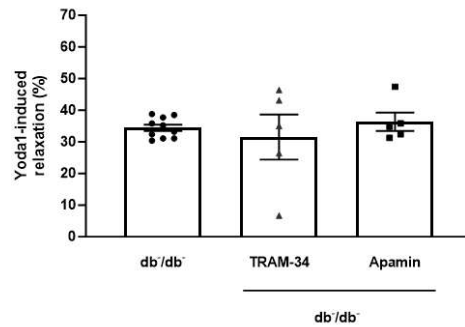


**Figure 9.** Effects of  $IK_{Ca}$  and  $SK_{Ca}$  channel blockers on Yoda1-induced relaxation. Representative traces showing the relaxation induced by Yoda1 ( $10^{-5}$  M) after pre-treatment with TRAM-34 (A and B) and apamin (C and D) in control and  $db^{-}/db^{-}$  mice. The data in E and F represent the mean  $\pm$  SEM values of Yoda1-induced relaxation observed in the experiments.  $n = 5$  for control (TRAM-34),  $n=5$  for  $db^{-}/db^{-}$  (TRAM-34),  $n = 5$  for control (apamin),  $n = 5$  for  $db^{-}/db^{-}$  (apamin). \* $p < 0.05$  vs. control, # $p < 0.05$  vs.  $db^{-}/db^{-}$ . TRAM-34, Triarylmethane-34;  $IK_{Ca}$ , intermediate-conductance  $Ca^{2+}$ -activated  $K^{+}$  channel;  $SK_{Ca}$ , small-conductance  $Ca^{2+}$ -activated  $K^{+}$  channel; W/O, wash out.

### **8. Effect of BK<sub>Ca</sub> channel blocker on Yoda1-induced relaxation**

To confirm the involvement of the BK<sub>Ca</sub> channel in Yoda1-induced relaxation, we conducted studies using both endothelium-intact and endothelium-denuded mesenteric arteries. In control mice, pre-treatment with charybdotoxin (ChTX,  $5 \times 10^{-8}$  M), a BK<sub>Ca</sub> channel blocker, significantly reduced Yoda1-induced relaxation in endothelium-intact arteries (non-treated:  $40.9 \pm 0.8\%$ , ChTX-treated:  $18.5 \pm 1.3\%$ ; Fig. 10A). However, pre-treatment with ChTX did not affect Yoda1-induced relaxation in endothelium-denuded arteries in control mice (Fig. 10B). In contrast, Yoda1-induced relaxation was significantly inhibited by ChTX, not only in endothelium-intact arteries but also in endothelium-denuded arteries in db<sup>-</sup>/db<sup>-</sup> mice. In endothelium-intact arteries in db<sup>-</sup>/db<sup>-</sup> mice, pre-treatment with ChTX reduced Yoda1-induced relaxation from  $34.4 \pm 1.0\%$  to  $12.4 \pm 3.9\%$  (approximately 22% reduction, Fig. 10C). In endothelium-denuded arteries in db<sup>-</sup>/db<sup>-</sup> mice, pre-treatment with ChTX reduced Yoda1-induced relaxation from  $23.7 \pm 2.2\%$  to  $11.3 \pm 5.1\%$  (approximately 12% reduction, Fig. 10D).

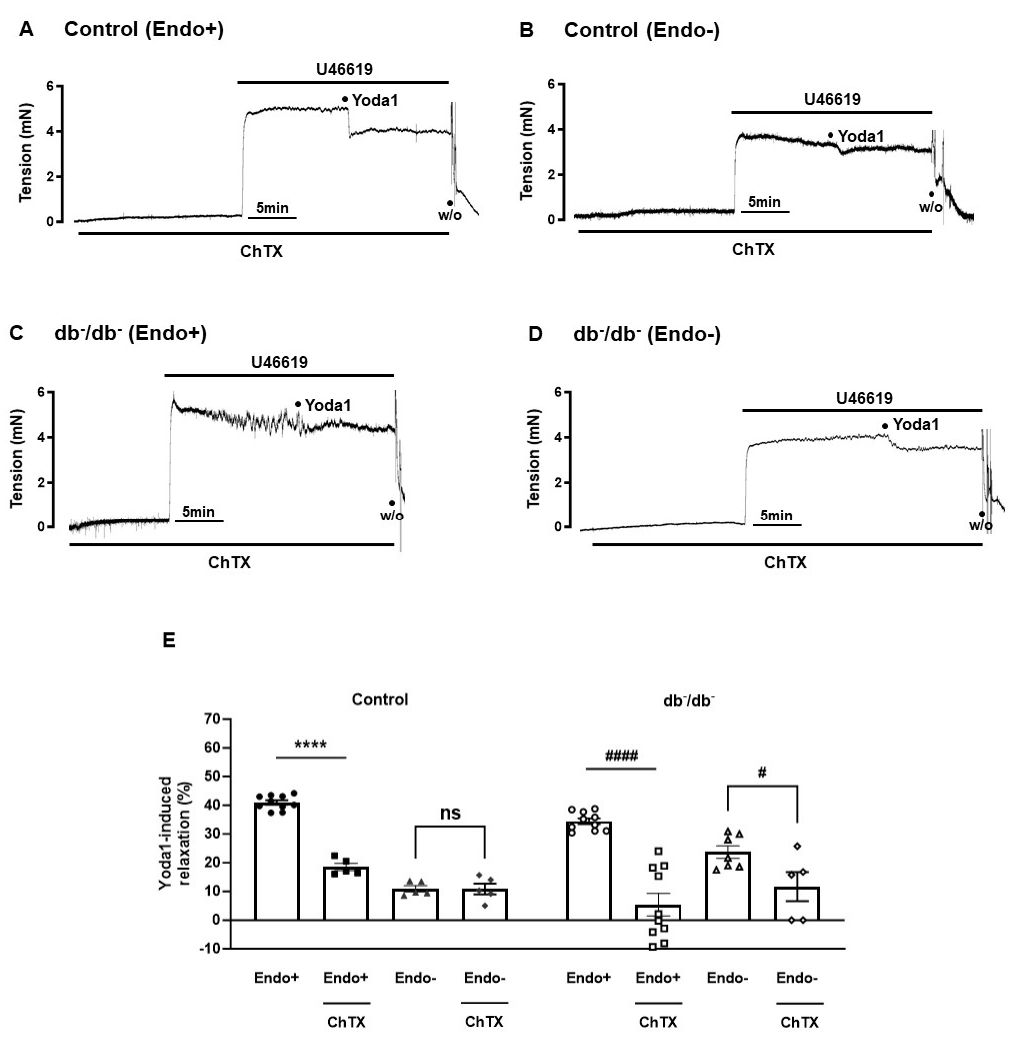


**Figure 10.** Effect of BK<sub>Ca</sub> channel blocker on Yoda1-induced relaxation. Representative traces showing the relaxation induced by Yoda1 (10<sup>-5</sup> M) after pre-treatment with ChTX (5x10<sup>-8</sup> M) in endothelium-intact and endothelium-denuded mesenteric arteries of control (A and B) and db<sup>-</sup>/db<sup>-</sup> mice (C and D). The data in E are presented as mean ± SEM values of Yoda1-induced relaxation observed in experiments. n=10 for control (Endo+), n=5 for control (Endo+) with ChTX, n=5 for control (Endo-), n=5 for control (Endo-) with ChTX, n=10 for db<sup>-</sup>/db<sup>-</sup> (Endo+), n=10 for db<sup>-</sup>/db<sup>-</sup> (Endo+) with ChTX, n=7 for db<sup>-</sup>/db<sup>-</sup> (Endo-), n=5 for db<sup>-</sup>/db<sup>-</sup> (Endo-) with ChTX. ns, no significant difference. \*\*\*\**p* < 0.0001, control (Endo+ and ChTX-) vs. control (Endo+ and ChTX+), #*p* < 0.05, db<sup>-</sup>/db<sup>-</sup> (Endo- and ChTX-) vs. db<sup>-</sup>/db<sup>-</sup> (Endo- and ChTX+), #####*p* < 0.0001, db<sup>-</sup>/db<sup>-</sup> (Endo+ and ChTX-) vs. db<sup>-</sup>/db<sup>-</sup> (Endo+ and ChTX+). ChTX, charybdotoxin; BK<sub>Ca</sub>, large-conductance Ca<sup>2+</sup>-activated K<sup>+</sup> channel; W/O, wash out.

### **9. Expression of BK<sub>Ca</sub> channel in mesenteric arteries of control and db<sup>-</sup>/db<sup>-</sup> mice**

As illustrated in Fig. 10E, a significant difference in the relaxation response to Yoda1 was observed between control and db<sup>-</sup>/db<sup>-</sup> mice when pre-treated with charybdotoxin (ChTX). Based on these results, we hypothesized that the BK<sub>Ca</sub> channel is involved in Yoda1-induced vascular relaxation in db<sup>-</sup>/db<sup>-</sup> mice. To explore the potential underlying mechanism, we compared the total protein expression level of the BK<sub>Ca</sub> channel in the mesenteric arteries of control and db<sup>-</sup>/db<sup>-</sup> mice. Our results showed no significant difference in the protein expression level of the BK<sub>Ca</sub> channel between the two groups (Fig. 11).

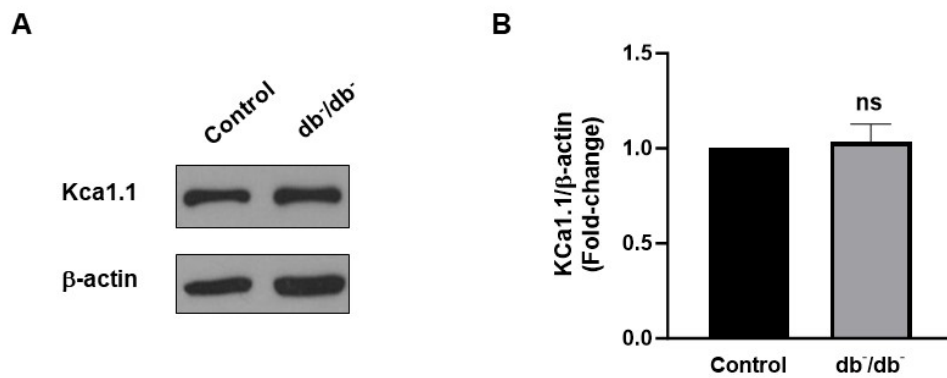
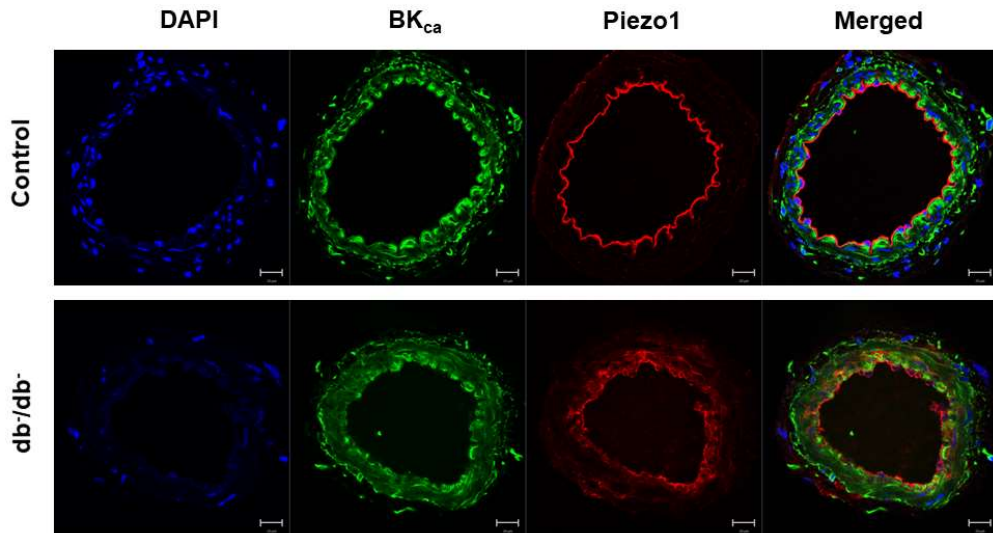


**Figure 11.** Expression level of BK<sub>Ca</sub> channel in mesenteric arteries of control and db/db<sup>-/-</sup> mice. Representative western blot (A) and semi-quantitative analysis (B) of protein level of K<sub>Ca</sub>1.1 (also called BK<sub>Ca</sub>) in mesenteric arteries of control and db/db<sup>-/-</sup> mice. Protein expression was normalized to  $\beta$ -actin and expressed as fold change relative to the control. The data are presented as mean  $\pm$  SEM (n=6).

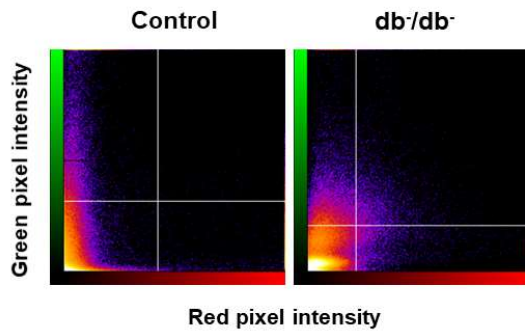
## **10. Co-localization of Piezo1 and BK<sub>Ca</sub> channel in mesenteric arteries of control and db<sup>-/-</sup>db<sup>-/-</sup> mice**

To investigate the concept of co-localization between Piezo1 and the BK<sub>Ca</sub> channel, we conducted double immunofluorescence staining followed by confocal analysis on the mesenteric arteries. Figure 9 illustrates that the staining for the anti-BK<sub>Ca</sub> channel overlaps with that of anti-Piezo1, indicating the presence of Piezo1 and the BK<sub>Ca</sub> channel in very close spatial positions in both groups (Fig 12A). Interestingly, the extent of co-localization was more pronounced in the db<sup>-/-</sup>db<sup>-/-</sup> mice (Fig. 12B). Statistical analysis revealed that the degree of co-localization was significantly higher in db<sup>-/-</sup>db<sup>-/-</sup> mice compared to control mice (Fig. 12C).

**A**



**B**



**C**

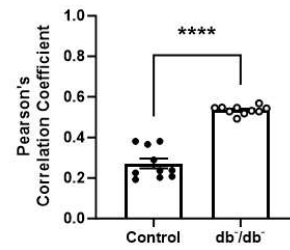


**Figure 12.** Co-localization of Piezo1 channels and BK<sub>Ca</sub> channels in mesenteric arteries of control and db<sup>-</sup>/db<sup>-</sup> mice. Representative images (A) of co-immunofluorescence staining of BK<sub>Ca</sub> (green), Piezo1 (red), and DAPI (nuclei, blue). Scatter plot (B) of intensity level in each channel; green is shown on the x-axis and red is shown on the y-axis. The degree of co-localization was quantified and compared using Pearson's correlation coefficient (C). The data are presented as mean ± SEM. \*\*\*\* $p < 0.0001$ , control vs. db<sup>-</sup>/db<sup>-</sup>.

#### IV. DISCUSSION

Endothelial dysfunction is a hallmark of diabetes and plays a pivotal role in the development of vascular complications.<sup>14</sup> In a previous study, we reported impaired endothelium-dependent relaxation (EDR) in mesenteric arteries of db<sup>-</sup>/db<sup>-</sup> mice.<sup>15</sup> Here, we confirmed reduced ACh-induced EDR in mesenteric arteries of type 2 diabetic (db<sup>-</sup>/db<sup>-</sup>) mice compared to C57BL/6 (control) mice (Fig. 2). Piezo1 is a non-selective cation channel activated by mechanical stimuli, including pressure, shear stress, and membrane tension.<sup>16</sup> This channel is permeable to cations such as Na<sup>+</sup>, K<sup>+</sup>, Ca<sup>2+</sup>, and Mg<sup>2+</sup>, with a particular preference for Ca<sup>2+</sup>.<sup>17</sup> Chemical activators such as Yoda1 are often used to investigate Piezo1 activation, as they have been shown to open Piezo1 channels and promote Ca<sup>2+</sup> influx across synthetic cell membranes.<sup>18</sup> Piezo1 plays a significant role in vascular tone regulation.<sup>19</sup> Activation of Piezo1 in the vasculature leads to an increase in intracellular calcium levels ([Ca<sup>2+</sup>]<sub>i</sub>), which subsequently activates endothelial nitric oxide synthase (eNOS) through specific signaling pathways. This cascade results in the production of endothelial nitric oxide (NO), leading to vasodilation.<sup>18,20</sup> However, despite the importance of Piezo1 in vascular function, there have been no studies on the involvement of Piezo1 in the mesenteric resistance arteries of type 2 diabetic mice (db<sup>-</sup>/db<sup>-</sup>).

Our study revealed that the concentration-dependent relaxation response induced by Yoda1 was reduced in the mesenteric resistance arteries of db<sup>-</sup>/db<sup>-</sup> mice compared to control mice (Fig. 3 and 4), which was associated with a reduction in Piezo1 expression levels (Fig. 1). The specificity of the Piezo1 activator Yoda1 was confirmed by the significant reduction in the relaxation response when pre-treated with the selective inhibitor Dooku1 (a selective inhibitor of Yoda1) and the mechanosensitive channel-selective inhibitor GsMTx4 (Fig. 7). We further explored the mechanisms underlying

Piezol activation-induced relaxation. The vascular endothelium, situated between circulating blood and vascular smooth muscle, plays a critical role in regulating vascular tone. Interestingly, the removal of the endothelium reduced the relaxation responses induced by Yoda1 in both control and  $db^{-}/db^{-}$  mice, indicating that the endothelium contributes to Yoda1-induced relaxation (Fig. 3 and 4). However, the degree of reduction was significantly greater in control mice than in  $db^{-}/db^{-}$  mice, suggesting that an endothelium-dependent mechanism is more prominently involved in control mice than in  $db^{-}/db^{-}$  mice. The endothelium is known to release various vasodilator factors, including nitric oxide (NO), prostacyclin ( $PGI_2$ ), and endothelium-derived hyperpolarizing factors (EDHF), in response to various stimuli.<sup>21</sup> Among them, NO is a potent endothelium-derived relaxing factor that plays a crucial role in regulating vascular tone. It is synthesized from L-arginine and oxygen through the enzymatic action of endothelial nitric oxide synthase (eNOS). Once produced, NO diffuses into vascular smooth muscle cells, where it activates soluble guanylate cyclase (sGC), leading to the production of guanosine 3',5'-cyclic monophosphate (cGMP). Elevated cGMP levels result in the relaxation of vascular smooth muscle.<sup>22,23</sup> Our experiments demonstrated that pre-treatment with the NO synthase inhibitor ( $N^{\omega}$ -Nitro-L-arginine, L-NNA) and the sGC inhibitor, 1H-[1,2,4]oxadiazolo [4,3,-a] quinoxalin-1-one (ODQ), attenuated Yoda1-induced relaxation in both groups, indicating the involvement of NO/cGMP signaling in this response (Fig. 8). Another important vasodilator produced by the endothelium is prostacyclin ( $PGI_2$ ).  $PGI_2$  is a prostanoid synthesized from arachidonic acid through enzymatic activity in the cyclooxygenase (COX) pathway.  $PGI_2$  promotes the relaxation of vascular smooth muscle by activating adenylate cyclase, leading to the production of adenosine 3',5'-cyclic monophosphate (cAMP). Elevated cAMP levels reduce intracellular calcium concentrations, resulting in vascular smooth muscle relaxation.<sup>24,25</sup> However, our

experiments demonstrated that pre-treatment with the COX inhibitor, indomethacin, did not have a significant effect on Yoda1-induced relaxation in both control and db<sup>-</sup>/db<sup>-</sup> mice. This suggests that PGI<sub>2</sub> production may not be a major contributor to the observed Yoda1-induced relaxation (Fig. 8).

The regulation of vascular tone is complex and involves various mechanisms, including the activity of K<sup>+</sup> channels, particularly Ca<sup>2+</sup>-activated K<sup>+</sup> channels (K<sub>Ca</sub>). In the vascular wall, there are three subtypes of calcium-activated potassium channels: large-conductance (BK<sub>Ca</sub>), intermediate-conductance (IK<sub>Ca</sub>), and small-conductance (SK<sub>Ca</sub>) channels. Intriguingly, our observations suggest that IK<sub>Ca</sub> and SK<sub>Ca</sub> channels play a partial role in Yoda1-induced relaxation in control mice, as pre-treatment with their respective blockers, TRAM-34 and apamin, resulted in some inhibition of the relaxation response. However, in db<sup>-</sup>/db<sup>-</sup> mice, pre-treatment with TRAM-34 and apamin did not significantly affect Yoda1-induced relaxation (Fig. 9). To investigate the involvement of the BK<sub>Ca</sub> channel, we treated endothelium-intact and -denuded arteries with charybdotoxin (ChTX), a BK<sub>Ca</sub> channel blocker. ChTX treatment significantly reduced Yoda1-induced relaxation in endothelium-intact arteries in both control and db<sup>-</sup>/db<sup>-</sup> mice. Interestingly, in endothelium-denuded arteries, Yoda1-induced relaxation was markedly inhibited by ChTX only in db<sup>-</sup>/db<sup>-</sup> mice (Fig. 10). This suggests that the BK<sub>Ca</sub> channel in smooth muscle cells may play a more significant role in Yoda1-induced relaxation in db<sup>-</sup>/db<sup>-</sup> mice. In turn, these data suggest that BK<sub>Ca</sub>, IK<sub>Ca</sub>, and SK<sub>Ca</sub> channels could be involved in Yoda1-induced relaxation in control mice, whereas only the BK<sub>Ca</sub> channel plays a significant role in db<sup>-</sup>/db<sup>-</sup> mice. Despite the low expression of Piezo1 in db<sup>-</sup>/db<sup>-</sup> mice, as shown in Figure 1, and no difference in BK<sub>Ca</sub> channel expression (Fig. 11), the decrease in Yoda1-induced relaxation by ChTX treatment was greater in db<sup>-</sup>/db<sup>-</sup> mice. Therefore, we hypothesized that the association between the BK<sub>Ca</sub> channel and Piezo1 would be more pronounced in db<sup>-</sup>/db<sup>-</sup>

mice. Intriguingly, the immunofluorescence staining and confocal analysis data further supported that Piezo1 and the BK<sub>Ca</sub> channel are structurally closer together in db<sup>-</sup>/db<sup>-</sup> mice (Fig. 12). We speculate that an increase in co-localization of Piezo1 and BK<sub>Ca</sub> may serve as a compensatory mechanism in response to the reduced Piezo1 expression observed in db<sup>-</sup>/db<sup>-</sup> mice. The present study is the first report on the distinct aspects of vascular response induced by Piezo1 activation in the mesenteric resistance arteries of db<sup>-</sup>/db<sup>-</sup> mice. Our findings could thus provide novel insights into identifying the potential mechanisms contributing to vascular dysfunction in diabetes.

## V. CONCLUSION

The present study demonstrates that Piezo1 activation by its specific agonist, Yoda1, induces concentration-dependent relaxation in mesenteric resistance arteries in both control and db<sup>-</sup>/db<sup>-</sup> mice. This response is mediated through both endothelium-dependent and -independent mechanisms. In control mice, Yoda1-induced vascular relaxation is greater than in db<sup>-</sup>/db<sup>-</sup> mice and is primarily endothelium-dependent. Moreover, in control mice, IK<sub>Ca</sub>, SK<sub>Ca</sub>, and BK<sub>Ca</sub> channels are involved in Yoda1-induced relaxation. However, in db<sup>-</sup>/db<sup>-</sup> mice, Yoda1-induced relaxation is slightly reduced by endothelial denudation, and only the BK<sub>Ca</sub> channel blocker significantly reduces Yoda1-induced relaxation. Additionally, the co-localization of BK<sub>Ca</sub> and Piezo1 was increased in db<sup>-</sup>/db<sup>-</sup> mice. These results indicate that Yoda1-induced vascular relaxation in db<sup>-</sup>/db<sup>-</sup> mice is mainly caused by the BK<sub>Ca</sub> channel present in vascular smooth muscle cells.

In healthy conditions, activation of Piezo1 primarily results in endothelium-dependent vascular relaxation. However, in type 2 diabetes, characterized by endothelial cell damage occurs, it is hypothesized that Piezo1 induces vascular relaxation by engaging vascular smooth muscle cells instead. These characteristics will provide important knowledge for the development of treatments for diabetic complications and vascular dysfunction targeting Piezo1.

## REFERENCES

1. N.M. Ivers, M. Jiang, J. Alloo, A. Singer, D. Ngui, C.G. Casey, et al., Diabetes Canada 2018 clinical practice guidelines: Key messages for family physicians caring for patients living with type 2 diabetes. *Can Fam Physician*. 2019; 65 (1) :14-24.
2. Y. Shi, D.D. Ku, R.Y. Man, P.M. Vanhoutte, Augmented endothelium-derived hyperpolarizing factor-mediated relaxations attenuate endothelial dysfunction in femoral and mesenteric, but not in carotid arteries from type I diabetic rats. *J Pharmacol Exp Ther*. 2006; 318 (1): 276-81.
3. G.X. Shen, Oxidative stress and diabetic cardiovascular disorders: roles of mitochondria and NADPH oxidase. *Can J Physiol Pharmacol*. 2010; 88 (3): 241-48.
4. X. Liu, F. Nakamura, Mechanotransduction, nanotechnology, and nanomedicine. *J Biomed Res*. 2020; 35 (4): 284-93.
5. M. Costigan, J. Scholz, C.J. Woolf, Neuropathic pain: a maladaptive response of the nervous system to damage. *Annu Rev Neurosci*. 2009; 32: 1-32.
6. K. Retailleau, F. Duprat, M. Arhatte, S.S. Ranade, R. Peyronnet, J.R. Martins, et al., Piezo1 in smooth muscle cells is involved in hypertension-dependent arterial remodeling. *Cell Rep*. 2015; 13 (6):1161-71.
7. R. Emig, W. Knodt, M.J. Krussig, C.M. Zgierski-Johnston, O. Gorka, O. Gross, et al., Piezo1 channels contribute to the regulation of human atrial fibroblast mechanical properties and matrix stiffness sensing. *Cells*. 2021; 10 (3): 633.
8. F. Jiang, K. Yin, K. Wu, M. Zhang, S. Wang, H. Cheng, et al., The mechanosensitive Piezo1 channel mediates heart mechano-chemo transduction. *Nat Commun*. 2021; 12 (1): 869.

9. S.S. Ranade, Z. Qiu, S.H. Woo, S.S. Hur, S.E. Murthy, S.M. Cahalan, et al., Piezo1, a mechanically activated ion channel, is required for vascular development in mice. *Proc Natl Acad Sci U S A*. 2014; 111 (28): 10347-52.
10. D. Choi, E. Park, E. Jung, B. Cha, S. Lee, J. Yu, et al., Piezo1 incorporates mechanical force signals into the genetic program that governs lymphatic valve development and maintenance. *JCI Insight*. 2019; 4 (5): e125068
11. T. Porto Ribeiro, S. Barbeau, I. Baudrimont, P. Vacher, V. Freund-Michel, G. Cardouat, et al., Piezo1 channel activation reverses pulmonary artery vasoconstriction in an early rat model of pulmonary hypertension: The role of Ca(2+) influx and Akt-eNOS pathway. *Cells*. 2022; 11 (15): 2349
12. D. Douguet, A. Patel, A. Xu, P.M. Vanhoutte, E. Honore, Piezo ion channels in cardiovascular mechanobiology *Mechanobiology. Trends Pharmacol Sci*. 2019; 40 (12): 956-70.
13. W. Zhu, S. Guo, M. Homilius, C. Nsubuga, S.H. Wright, D. Quan, et al., PIEZO1 mediates a mechanothrombotic pathway in diabetes. *Sci Transl Med*. 2022; 14 (626): eabk1707.
14. F. Cosentino, T.F. Luscher, Endothelial dysfunction in diabetes mellitus. *J Cardiovasc Pharmacol*. 1998; 32 (3): S54-61.
15. S.K. Choi, Y. Kwon, S. Byeon, C.E. Haam, Y.H. Lee, AdipoRon, adiponectin receptor agonist, improves vascular function in the mesenteric arteries of type 2 diabetic mice. *PLoS One*. 2020; 15 (3): e0230227.
16. B. Dienes, T. Bazso, L. Szabo, L. Csernoch, The role of the Piezo1 mechanosensitive channel in the musculoskeletal system. *Int J Mol Sci*. 2023; 24 (7): 6513.
17. B. Coste, J. Mathur, M. Schmidt, T.J. Earley, S. Ranade, M.J. Petrus, *et al.*,

- Piezo1 and Piezo2 are essential components of distinct mechanically activated cation channels. *Science*. 2010; 330 (6000): 55-60.
18. D.J. Beech, A.C. Kalli, Force sensing by piezo channels in cardiovascular health and disease. *Arterioscler Thromb Vasc Biol*. 2019; 39 (11): 2228-39.
  19. X.Z. Fang, T. Zhou, J.Q. Xu, Y.X. Wang, M.M. Sun, Y.J. He, *et al.*, Structure, kinetic properties and biological function of mechanosensitive Piezo channels. *Cell Biosci*. 2021; 11 (1): 13.
  20. J. Wu, A.H. Lewis, J. Grandl, Touch, Tension, and Transduction - The Function and regulation of Piezo ion channels. *Trends Biochem Sci*. 2017; 42 (1): 57-71.
  21. J.B. Su, Vascular endothelial dysfunction and pharmacological treatment. *World J Cardiol*. 2015; 7 (11): 719-41.
  22. S. Moncada, R.M. Palmer, E.A. Higgs, Nitric oxide: physiology, pathophysiology, and pharmacology. *Pharmacol Rev*. 1991; 43 (2): 109-42.
  23. R.M. Palmer, D.S. Ashton, S. Moncada, Vascular endothelial cells synthesize nitric oxide from L-arginine. *Nature*. 1988; 333 (6174): 664-66.
  24. J.R. Vane, R.M. Botting, Pharmacodynamic profile of prostacyclin. *Am J Cardiol*. 1995; 75 (3): 3A-10A.
  25. J.R. Vane, E.E. Anggard, R.M. Botting, Regulatory functions of the vascular endothelium. *N Engl J Med*. 1990; 323 (1): 27-36.

## 당뇨 쥐와 정상 쥐의 장간막동맥에서 피에조1 활성화로 유도된 혈관 이완의 비교

<지도교수 이영호>

연세대학교 대학원 의학과

함채은

기계적인 자극에 민감한 이온 통로인 피에조1은 혈관의 생리학적 기능 및 질병 발생에 중요한 역할을 하지만, 당뇨병에서 나타나는 혈관 기능 이상에서 피에조1의 활성화 기전은 명확하게 밝혀지지 않았다. 따라서, 본 연구에서는 피에조1의 활성화로 유도된 혈관 반응을 확인하고, 제 2형 당뇨 쥐와 정상 쥐의 장간막동맥에서 피에조1 활성화로 유도되는 이완 기전의 차이를 규명하고자 연구를 수행하였다. 당뇨 쥐에서는 내피세포가 손상된 것으로 나타났으며, 피에조1 단백질의 발현은 정상 쥐보다 당뇨 쥐에서 발현이 유의하게 감소된 것으로 나타났다. 피에조1 작용제인 Yoda1은 정상 쥐와 당뇨 쥐 모두에서 농도 의존적으로 혈관의 이완을 유도하였으며, 정상 쥐와 비교하여 당뇨 쥐에서 이완 반응의 크기가 유의하게 감소된 것으로 나타났다. 내피세포가 제거된 혈관에서 Yoda1에 의해 유도된 이완 반응의 크기는 두 그룹 모두에서 유의하게 감소된 것으로 나타났으며, 당뇨 쥐보다 정상 쥐에서 이완의 크기가 유의하게 감소된 것으로 나타났다. 내피세포가 온전한 혈관에서 Yoda1의 혈관 이완 효과는 L-NNA와 ODQ의 전처치로 인하여 이완 효과가 두 그룹에서 유의하게 억제된 것으로 나타났다. 정상 쥐의 내피세포가

온전한 혈관에서 apmain, TRAM-34 및 ChTX의 전처치는 Yoda1으로 유도된 혈관 이완을 억제시킨 것으로 나타났다. 한편, 당뇨 쥐의 내피세포가 제거된 혈관에서 ChTX의 전처치는 Yoda1의 이완의 크기를 유의하게 감소시킨 것으로 나타났으나, 정상 쥐에서는 Yoda1에 이완 효과에 영향을 주지 않는 것으로 보여진다. 공동-면역형광 분석 결과, 두 그룹 모두에서 전도도가 큰 칼슘 의존성 포타슘 통로 ( $BK_{Ca}$ ) 통로와 피에조1 통로의 공동 발현을 보여주었다. 피어슨 상관 계수로 두 통로의 발현 상관관계를 측정한 결과, 정상 쥐보다 당뇨 쥐에서 공동 발현이 증가된 것으로 보여지며, 이는 당뇨 쥐에서 구조적 결합이 더 많다는 것을 나타낸다. 즉, 당뇨 쥐에서는 내피세포의 기능이 손상되어있기 때문에 보상기전으로 평활근 세포에 존재하는 전도도가 큰 칼슘 의존성 포타슘 통로의 활성화를 통해 혈관을 이완시키는 것으로 설명될 수 있다. 본 연구는 제 2형 당뇨 쥐의 장간막동맥에서 피에조1 활성화로 유도된 혈관 이완 기전이 정상 쥐와 다르다는 것을 규명한 첫번째 연구로, 이상의 결과들은 당뇨병에서 나타나는 혈관 기능 이상에 기여하는 잠재적인 기전을 확인하는데 유용한 기초자료를 제공할 것으로 기대된다.

---

핵심되는 말: 피에조1; yoda1; 제2형 당뇨병; 혈관 이완, 기계신호전달

## PUBLICATION LIST

1. **Haam, C.E.**, Byeon, S., Choi, S., Oh, E.Y, Choi, S-K., & Lee, Y-H. Vasorelaxant Effect of *Trachelospermi caulis* Extract on Rat Mesenteric Resistance Arteries. *Molecules*. 2022;27(16):5300
2. **Haam, C.E.**, Byeon, S., Choi, S.J., Lim, S., Choi, S-K., & Lee, Y-H. Vasodilatory Effect of *Alpinia officinarum* Extract in Rat Mesenteric Arteries. *Molecules*. 2022;27(9):2711
3. Choi, S., **Haam, C.E.**, Byeon, S., Oh, E., Choi, S-K, & Lee, Y-H. Investigating the Cardiovascular Benefits of Dapagliflozin: Vasodilatory Effect on Isolated Rat Coronary Arteries. *Int. J. Mol. Sci.* 2023; 24(23): 16873
4. Oh, E.Y., **Haam, C.E.**, Choi, S., Byeon, S., Choi, S-K., & Lee, Y-H. Ezetimibe Induces Vasodilation in Rat Mesenteric Resistance Arteries through Inhibition of Extracellular Ca<sup>2+</sup> Influx. *Int. J. Mol. Sci.* 2023; 24(18): 13992
5. Choi, S., **Haam, C.E.**, Oh, E., Byeon, S., Choi, S-K, & Lee, Y-H. Vanillin Induces Relaxation in Rat Mesenteric Resistance Arteries by Inhibiting Extracellular Ca<sup>2+</sup> Influx. *Molecules*. 2023; 28(1): 288
6. Kwon, Y., **Haam, C.E.**, Byeon, S., Choi, S-K, & Lee, Y-H. Effects of 3-methyladenine, an autophagy inhibitor, on the elevated blood pressure and arterial dysfunction of angiotensin II-induced hypertensive mice. *Biomedicine & pharmacotherapy*. 2022; 154: 113588
7. Lee, M.Y., **Haam, C.E.**, Mun, J., Lim, G., Lee, B.H., & Oh, K. Development of a FOXM1-DBD Binding Assay for High-Throughput Screening Using TR-FRET Assay. *Biological & pharmaceutical bulletin*. 2021; 44 (10): 1484-91

8. Kwon, Y., **Haam, C.E.**, Byeon, S., Choi, S.J., Shin, D., Choi, S-K, & Lee, Y-H. Vasodilatory Effect of *Phellinus linteus* Extract in Rat Mesenteric Arteries. *Molecules*, 2020; 25(14): 3160
9. Choi, S-K., Kwon, Y., Byeon, S., **Haam, C.E.**, & Lee, Y-H. AdipoRon, adiponectin receptor agonist, improves vascular function in the mesenteric arteries of type 2 diabetic mice. *PLoS ONE*, 2020; 15(3): e0230227